Letter

Clustering-induced localization of quantum walks on networks

Lucas Böttcher [1,2,*] and Mason A. Porter [3,4,5,†]

[1]*Department of Computational Science and Philosophy, Frankfurt School of Finance and Management, 60322 Frankfurt am Main, Germany*

[2]*Department of Medicine, University of Florida, Gainesville, Florida 32610, USA*

[3]*Department of Mathematics, University of California, Los Angeles, California 90095, USA*

[4]*Department of Sociology, University of California, Los Angeles, California 90095, USA*

[5]*Santa Fe Institute, Santa Fe, New Mexico 87501, USA*

(Received 5 December 2024; accepted 19 September 2025; published 1 December 2025)

Quantum walks on networks are a paradigmatic model in quantum information theory. Quantum-walk algorithms have been developed for various applications, including spatial-search problems, element-distinctness problems, and node-centrality analysis. Unlike their classical counterparts, the evolution of quantum walks is unitary, so they do not converge to a stationary distribution. However, for many applications, it is important to understand the long-time behavior of quantum walks and the impact of network structure on their evolution. In the present paper, we study localization of quantum walks on networks. We demonstrate how localization emerges in highly clustered networks that we construct by recursively attaching triangles, and we derive an analytical expression for the long-time inverse participation ratio that depends on products of eigenvectors of the quantum-walk Hamiltonian. Building on the insights from this example, we then show that localization also occurs in Kleinberg navigable small-world networks and Holme–Kim power-law cluster networks. Our results illustrate that local clustering, which is a key structural feature of networks, can induce localization of quantum walks.

DOI: 10.1103/pp6q-n7mx

Quantum walks have numerous and diverse applications, including spatial-search problems [1–4], element-distinctness problems [5], and node-centrality analysis [6–12]. Potential applications of quantum walks extend well beyond these examples, as any problem that can be solved by a general-purpose quantum computer can also be implemented as a quantum walk on a network [13,14]. Quantum walks are also effective models of various transport processes, such as energy transport in photosynthetic complexes [15,16], and they provide a useful framework to examine relationships between structural and dynamical features in quantum networks [17]. Unlike classical random walks, quantum walks evolve unitarily and thus do not converge to a stationary distribution [18]. To mathematically characterize the evolution of quantum walks, one usually considers long-time means of quantities such as occupation probabilities and transition probabilities. Examining the long-time behavior of quantum walks and the influence of network structure on their evolution can help guide the integration of quantum walks into algorithms [19].

In the present paper, we study *localization* of continuous-time quantum walks (CTQWs) on networks. Localization refers to the tendency of a dynamical process on a network to eventually be confined to a small set of nodes [20–25]. It arises from the interplay between a network's structural properties and a dynamical process on it.

Prior research on CTQWs has illustrated that adding edges uniformly at random to a ring network with nearest-neighbor connections is associated with ensemble-averaged transition probabilities that are large for an initially excited node (i.e., a single node that is initially occupied) and close to 0 for the other nodes [26]. Individual realizations of quantum walks on such networks do not exhibit localization. However, when one averages transition probabilities across many realizations of this random edge-addition process, the resulting averages of the transitions between different nodes tend to cancel each other, so an initial excitation of one node remains localized on average in its initial location. Researchers have observed localization of individual quantum walks in tree networks with Hamiltonians that incorporate disorder [27,28]. Other researchers have linked certain local connectivity patterns that arise from 0 eigenvalues with quantum-walk localization [29]. It is also known that quadratic perturbations can induce localization of quantum walks in certain situations [30].

There is also a body of work on discrete-time quantum walks on networks [31–42]. These studies include many papers on localization that involve both various lattices (and a fractal network) and "coin operators", which act on the spin component of an underlying product state.

To study localization of CTQWs on networks, we first establish how localization emerges in highly clustered networks that we construct by recursively attaching triangles. We then build on this example to show that localization also occurs in Kleinberg navigable small-world networks [43] and Holme–Kim power-law cluster networks [44]. These localization effects have potential implications for the use of quantum walks in quantum memory, where localized walks help reduce the size of the position space that is needed to store information [45]. Our results also illustrate

*Contact author: l.boettcher@fs.de

†Contact author: mason@math.ucla.edu

how structural characteristics of networks can suppress the speed-up of quantum-walk propagation over classical-walk propagation on networks. It is relevant to consider this issue when employing quantum walks in quantum communication channels [27].

Quantum walks on networks. We consider unweighted, undirected networks in the form of graphs $G = (V, E)$, where V is a set of nodes and E is a set of edges. The number of nodes is $N = |V|$, and the number of edges is $M = |E|$. We describe the edges between nodes using an adjacency matrix $A \in \{0, 1\}^{N\times N}$. The entry a_{ij} of the matrix A is 1 if nodes i and j are adjacent to each other and 0 if they are not. Because the network is undirected, $a_{ij} = a_{ji}$. The degree of a node i is $k_i = \sum_{j=1}^{N} a_{ij}$. Unless we state otherwise, we do not consider self-edges (i.e., we set $a_{ii} = 0$). The mean clustering coefficient of an undirected network G is $C(G) = N^{-1} \sum_{i=1}^{N} c_i$, where the local clustering coefficient of node i is $c_i = \sum_{j,k} a_{ij}a_{jk}a_{ki}/(k_i(k_i - 1))$ for $k_i \geqslant 2$ and $c_i = 0$ otherwise [46].

The wave function $|\psi\rangle \in \mathbb{C}^N$ of a CTQW evolves according to the Schrödinger equation

$$\frac{\mathrm{d}}{\mathrm{d}t}\,|\psi(t)\rangle = -\mathrm{i}H\,|\psi(t)\rangle\,, \tag{1}$$

where $\mathrm{i} = \sqrt{-1}$ is the imaginary unit and the Hamiltonian H is the infinitesimal generator of time translation. We assume the normalization $\langle\psi(t)|\psi(t)\rangle = 1$. In accordance with Refs. [9,10,47], we let H be the symmetric and normalized graph Laplacian matrix. That is,

$$H = D^{-1/2}LD^{-1/2}\,, \tag{2}$$

where $D = \sum_{j=1}^{N} k_j\,|j\rangle\langle j|$ is the degree matrix and $L = D - A$ is the combinatorial graph Laplacian matrix. The quantity $|j\rangle \in \mathbb{C}^N$ is an orthonormal basis vector that satisfies $\langle i|j\rangle = \delta_{ij}$, where δ_{ij} denotes the Kronecker delta, which is 1 if $|i\rangle = |j\rangle$ and is 0 otherwise. For the choice (2) of the Hamiltonian H, when a system is in the ground state, the probability that a quantum walk is on a given node is the same as in a classical random walk with the classical Hamiltonian LD^{-1} [47].

Localization measures. The probability that a CTQW with Hamiltonian H transitions from node j at time 0 to node i at time t is

$$\begin{aligned}\pi_{ij}(t) &= |\langle i|e^{-\mathrm{i}Ht}|j\rangle|^2 \\ &= \sum_{m=1}^{N} A_m^{ij} + \sum_{m<n} B_{mn}^{ij}\cos((\lambda_m - \lambda_n)t)\,,\end{aligned} \tag{3}$$

where

$$\begin{aligned}A_m^{ij} &:= |\langle i|e_m\rangle\langle e_m|j\rangle|^2, \\ B_{mn}^{ij} &:= 2\,\langle i|e_m\rangle\langle e_m|j\rangle\langle j|e_n\rangle\langle e_n|i\rangle\,.\end{aligned}$$

The quantities λ_m and e_m, respectively, are the eigenvalues and corresponding eigenvectors of H. That is, $He_m = \lambda_m e_m$. The long-time mean of the transition probability $\pi_{ij}(t)$ is

$$\bar{\pi}_{ij} = \lim_{T\to\infty}\frac{1}{T}\int_0^T \pi_{ij}(t)\,\mathrm{d}t\,. \tag{4}$$

Inserting Eq. (3) into Eq. (4) yields

$$\bar{\pi}_{ij} = \sum_{m=1}^{N} A_m^{ij} + \sum_{\substack{m<n,\\ \lambda_m=\lambda_n}} B_{mn}^{ij}\,. \tag{5}$$

To quantify the amount of localization of a CTQW, we calculate the inverse participation ratio (IPR) [48,49]

$$\mathrm{IPR}_j(t) = \sum_{i=1}^{N} |\langle i|e^{-\mathrm{i}Ht}|j\rangle|^4 = \sum_{i=1}^{N} \pi_{ij}^2(t) \tag{6}$$

that is associated with the initial state $|j\rangle$. To interpret the IPR, consider a wave function in which ℓ entries have magnitude $1/\sqrt{\ell}$ and $N - \ell$ entries have magnitude 0. This wave function has an IPR of $\ell(1/\sqrt{\ell})^4 = 1/\ell$. For a fully localized state, in which a CTQW is localized at a single node (i.e., $\ell = 1$), the IPR attains its maximum value of 1. For a fully delocalized state (i.e., $\ell = N$), the IPR attains its minimum value of $1/N$.

The long-time mean of $\mathrm{IPR}_j(t)$ is

$$\begin{aligned}\overline{\mathrm{IPR}}_j &= \lim_{T\to\infty}\frac{1}{T}\int_0^T \mathrm{IPR}_j(t)\,\mathrm{d}t \\ &= \sum_{i=1}^{N}\Bigg[\left(\sum_{m=1}^{N} A_m^{ij}\right)^2 + 2\sum_{m=1}^{N} A_m^{ij}\sum_{\substack{m<n,\\ \lambda_m=\lambda_n}} B_{mn}^{ij} \\ &\qquad + \sum_{\substack{m<n,\,r<s,\\ \lambda_m-\lambda_n=\lambda_r-\lambda_s}} C_{mnrs}^{ij} + \sum_{\substack{m<n,\,r<s,\\ \lambda_m-\lambda_n=\lambda_s-\lambda_r}} C_{mnrs}^{ij}\Bigg],\end{aligned} \tag{7}$$

where $C_{mnrs}^{ij} = B_{mn}^{ij}B_{rs}^{ij}/2$. The second term in the expression for $\overline{\mathrm{IPR}}_j$ quantifies localization due to degenerate eigenvalues, and the third and fourth terms quantify localization that is associated with eigenvalue quartets satisfying $\lambda_m - \lambda_n = \lambda_r - \lambda_s$ and $\lambda_m - \lambda_n = \lambda_s - \lambda_r$, respectively.

Localization in recursive triangle networks and related networks. We start by examining recursive triangle networks [see Fig. 1(a)]. These networks and related networks have also been studied in the framework of "network geometry with flavor" (NGF) [50–52] and in the context of hyperbolic lattices [53,54]. For a given depth d, recursive triangle networks have $N = 3 \times 2^d$ nodes and $M = 3 \times (2^{d+1} - 1)$ edges. In Fig. 1(a), we show such networks with depths of $d = 1$, $d = 2$, and $d = 3$. The mean clustering coefficients of these networks are 0.75, 0.71, and 0.70, respectively. For larger values of d, the mean clustering coefficient approaches a value of approximately 0.69.

For the recursive triangle networks with depths $d = 1$, $d = 2$, and $d = 3$, we show the long-time mean transition probabilities $\bar{\pi}_{ij}$ for all $i, j \in \{1, \ldots, N\}$ in Fig. 1(b). For depth $d = 1$, one can obtain analytical expressions for the eigenvalues and eigenvectors of the Hamiltonian (2). This enables one to write down the long-time mean

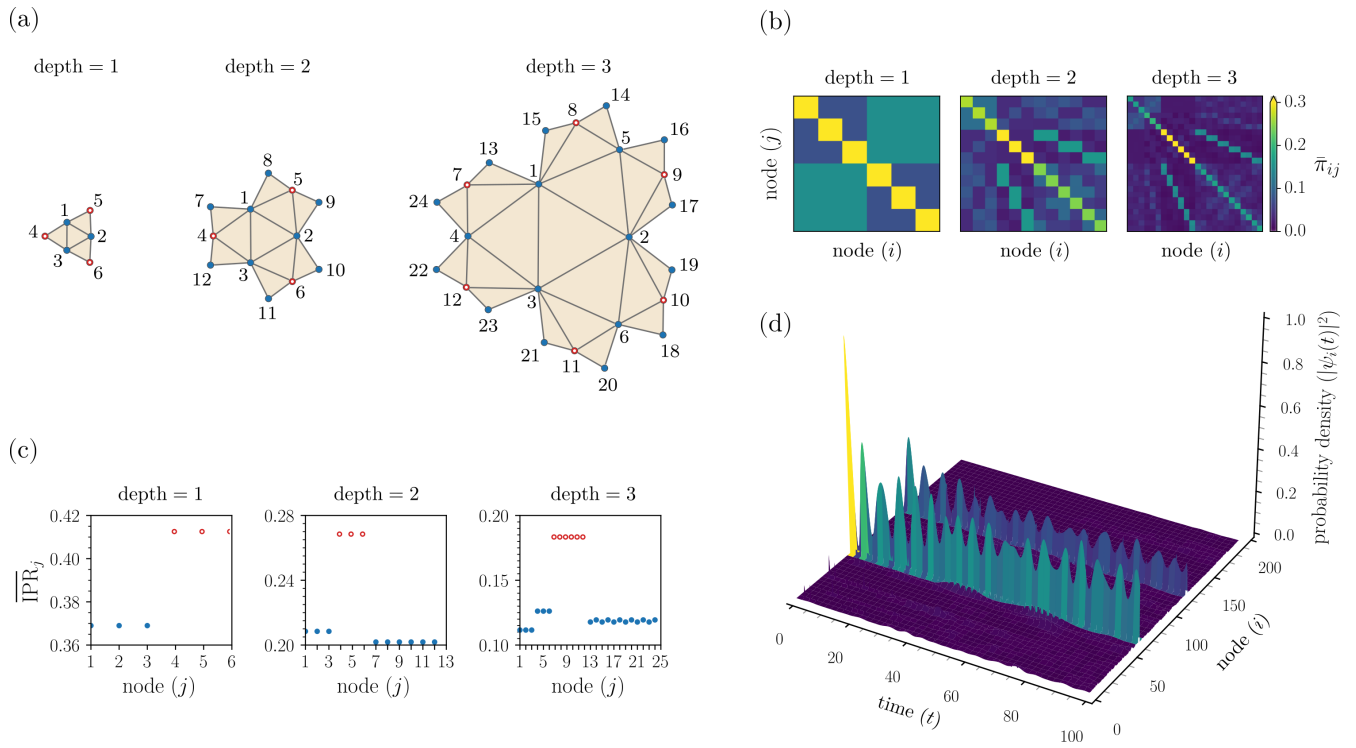

FIG. 1. Localization in recursive triangle networks. (a) Recursive triangle networks with depths 1, 2, and 3. The long-time mean inverse participation ratios (IPRs) of the nodes with hollow red circles are substantially larger than those of other nodes. (b) Long-time mean transition probabilities $\bar{\pi}_{ij}$ [see Eq. (4)] for the networks in panel (a). (c) Long-time mean IPR $\overline{\mathrm{IPR}}_j$ [see Eq. (7)] as a function of the initially excited node j. The hollow red circles indicate the maximum value of $\overline{\mathrm{IPR}}_j$. (d) Probability density $|\psi_i(t)|^2 = |\langle i|\psi(t)\rangle|^2$ as a function of the node i and time t for a CTQW that starts at node 61 in a recursive triangle network with depth 6. In this example, the quantum walk predominantly alternates between two nodes.

transition-probability matrix

$$\bar{\boldsymbol{\pi}}^{(d=1)} = \frac{1}{27}\begin{pmatrix} 11 & 2 & 2 & 4 & 4 & 4 \\ 2 & 11 & 2 & 4 & 4 & 4 \\ 2 & 2 & 11 & 4 & 4 & 4 \\ 4 & 4 & 4 & 11 & 2 & 2 \\ 4 & 4 & 4 & 2 & 11 & 2 \\ 4 & 4 & 4 & 2 & 2 & 11 \end{pmatrix}. \tag{8}$$

All diagonal entries $\bar{\pi}_{ii}^{(d=1)}$ have the same value and are noticeably larger than the off-diagonal entries $\bar{\pi}_{ij}^{(d=1)}$ (with $i \neq j$). This indicates that a CTQW that starts at node j has a higher probability of revisiting node j over a long time horizon than of occupying any other node. For recursive triangle networks with depths 2 and 3, over a long time horizon, CTQWs that start from nodes 4–6 and 7–12 [see Fig. 1(a)], respectively, have higher probabilities of revisiting these nodes than of occupying any other node [see Fig. 1(b)].

In Figs. 1(a) and 1(c), we highlight nodes with hollow red circles when their long-time mean IPRs [see Eq. (7)] are much larger than those of other nodes. For the recursive triangle network with depth $d = 1$, nodes 1–3 have a long-time mean IPR of $269/729 \approx 0.37$ and nodes 4–6 have a long-time mean IPR of $301/729 \approx 0.41$. For the recursive triangle networks with depths 2 and 3, the nodes with the largest long-time mean IPRs are those with the largest diagonal entries of $\bar{\pi}_{ij}$ in Fig. 1(b).

The Hamiltonian H of the recursive triangle network with depth $d = 1$ has eigenvalues 0, 3/4, 3/4, 3/2, 3/2, and 3/2. The degeneracies of the eigenvalues 3/4 and 3/2 are associated with contributions of the sums over B_{mn}^{ij} with $\lambda_m = \lambda_n$ [i.e., the second term in Eq. (7)]. The sums over C_{mnrs}^{ij} [i.e., the third and fourth terms in Eq. (7)] also contribute to the overall long-time mean IPR, as several eigenvalue quartets satisfy $\lambda_m - \lambda_n = \lambda_r - \lambda_s$ and $\lambda_m - \lambda_n = \lambda_s - \lambda_r$. We observe similar characteristics in recursive triangle networks with larger depths. For example, in those networks, the eigenvalue 3/2 is degenerate and is associated with contributions from the second term in Eq. (7). These results illustrate how localization is connected with both eigenvalue degeneracies and quartet spacings. It may also be useful to examine how localization relates to the spectral dimension, which has been used to link eigenvalue statistics with the behavior of dynamical processes on networks [55,56].

We also examine the absolute gap

$$\Delta\overline{\mathrm{IPR}} = \max_j(\overline{\mathrm{IPR}}_j) - \min_j(\overline{\mathrm{IPR}}_j) \tag{9}$$

and relative gap

$$\delta\overline{\mathrm{IPR}} = \frac{\max_j(\overline{\mathrm{IPR}}_j) - \min_j(\overline{\mathrm{IPR}}_j)}{\min_j(\overline{\mathrm{IPR}}_j)} \tag{10}$$

between the maximum and minimum long-time mean IPRs for recursive triangle networks with different depths. Consis-

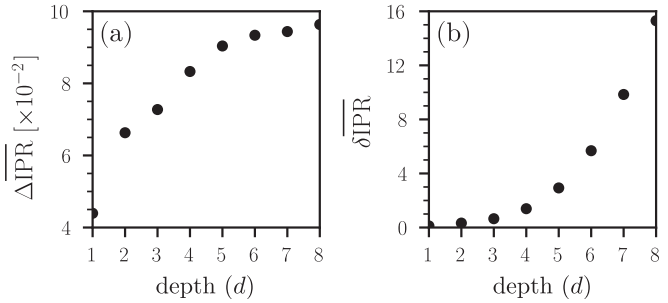

FIG. 2. Absolute and relative gaps between the maximum and minimum long-time mean IPRs for recursive triangle networks. (a) Absolute gap $\Delta\overline{\mathrm{IPR}}$ [see Eq. (9)] between the maximum and minimum long-time mean IPRs as a function of network depth d. (b) Relative gap $\delta\overline{\mathrm{IPR}}$ [see Eq. (10)] between the maximum and minimum long-time mean IPRs as a function of network depth d.

tent with the trend that we observed in Fig. 1(c), the values of both $\Delta\overline{\mathrm{IPR}}$ and $\delta\overline{\mathrm{IPR}}$ increase with the depth d (see Fig. 2). For $d = 1$, the absolute gap is $\Delta\overline{\mathrm{IPR}} \approx 0.04$ and the relative gap is $\delta\overline{\mathrm{IPR}} \approx 0.11$. By contrast, for $d = 8$, the absolute gap is $\Delta\overline{\mathrm{IPR}} \approx 0.10$ and the relative gap is $\delta\overline{\mathrm{IPR}} \approx 15.30$. The dependence of $\Delta\overline{\mathrm{IPR}}$ and $\delta\overline{\mathrm{IPR}}$ on the depth d in Fig. 2 suggests that the absolute and relative IPR gaps both approach a finite value as $d \to \infty$ but that $\min_j(\overline{\mathrm{IPR}}_j)$ approaches 0 as $d \to \infty$. For larger depths, some node excitations become highly localized, but others become increasingly delocalized.

As an example of a CTQW with substantial localization, we show the CTQW evolution on a recursive triangle network with depth 6 in Fig. 1(d). In this simulation, the CTQW starts at node 61 (of $3 \times 2^6 = 192$ nodes) and has $\overline{\mathrm{IPR}}_{61} \approx 0.11$. A closer examination of the probability-density oscillations reveals that the quantum walk predominantly alternates between two nodes.

For a discussion of recursive triangle networks with randomness (i.e., NGF networks), see *Appendix A: Localization in NGF networks*, where we illustrate that CTQWs still localize even in the presence of randomness.

Localization in other networks. To further study localization, we consider three additional types of networks: (i) Newman–Watts–Strogatz (NWS) small-world networks [57,58], (ii) Kleinberg navigable small-world networks [43] with a ring structure, and (iii) Holme–Kim (HK) power-law cluster networks [44]. In the NWS networks, each node is adjacent to its two nearest neighbors in a ring. For each edge (i, j), with probability p, one adds a new edge between node i and another node j' that one selects uniformly at random. In a Kleinberg network, edges that one adds to the backbone ring are more likely to connect nodes that are closer to each other (with respect to distance in the ring) than those that are farther apart from each other. When adding an edge, the probability of connecting two nodes i and j is proportional to $d(i, j)^{-\alpha}$, where $\alpha \geqslant 0$ is the clustering exponent[1] and $d(i, j)$

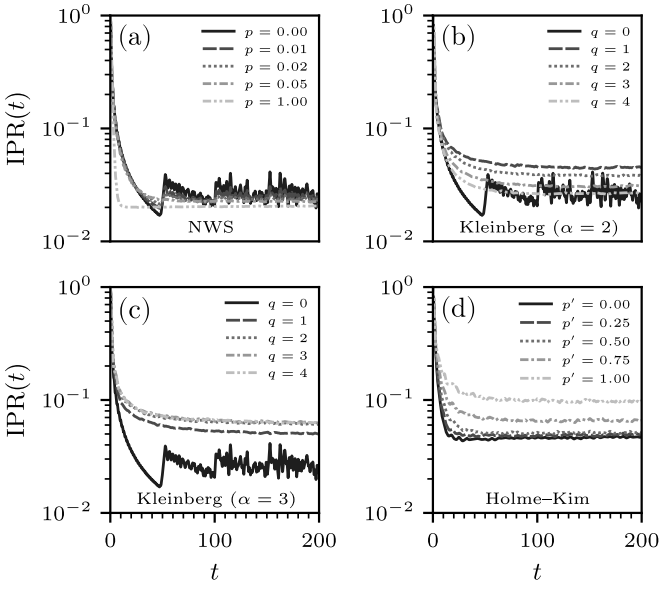

FIG. 3. Evolution of the IPR for several types of networks. (a) Newman–Watts–Strogatz (NWS) networks in which each node is adjacent to its two nearest neighbors in a ring. For each edge, the probabilities of adding a new edge are $p \in \{0, 0.01, 0.02, 0.05, 1\}$. (b, c) Kleinberg navigable small-world networks with clustering exponent α and $q \in \{0, 1, 2, 3, 4\}$ additional connections for each node. In panel (b), $\alpha = 2$; in panel (c), $\alpha = 3$. (d) Holme–Kim (HK) power-law cluster networks with probabilities $p' \in \{0, 0.25, 0.5, 0.75, 1\}$ of adding a triangle after adding a random edge. We construct an HK network by starting with an empty dyad (i.e., two isolated nodes) and iteratively adding new nodes until the network has 100 nodes. Each new node connects to two existing nodes using linear preferential attachment. All networks in panels (a)–(d) have $N = 100$ nodes, and all curves are means of results for 1000 networks. The CTQWs start at node 51.

is the geodesic distance between nodes i and j. (Observe that self-edges are possible.) The HK model is a generalization of the standard Barabási–Albert preferential-attachment model [46] that also adds triangles. One starts with an empty dyad (i.e., two isolated nodes). In each preferential-attachment step, one adds a new node and connects it to μ existing nodes (with $\mu = 2$ in this paper), which one chooses with probabilities that are proportional to their degrees. With probability p', for each new edge from the preferential-attachment step, one adds another edge and forms a triangle by connecting the new node to a neighbor (which one chooses uniformly at random) of the previously linked node. With probability $1 - p'$ (and also when it is not possible to form additional triangles with the new node), one instead performs a preferential-attachment step.

In Fig. 3, we plot IPR as a function of time for NWS, Kleinberg, and HK networks. We consider different model parameters and calculate means of results for 1000 networks. For the NWS networks, we consider the probabilities $p \in \{0, 0.01, 0.02, 0.05, 1\}$ and observe that the IPR approaches

[1]For $\alpha = 0$, one places edges uniformly at random. Increasing α biases edge placement toward connecting nearby nodes of a network, making it more likely that two neighbors of a node are also adjacent to each other and thereby increasing the network's mean clustering coefficient.

values between 0.02 and 0.03 [see Fig. 3(a)], corresponding to a delocalized wave function. The means of the mean clustering coefficients of the NWS networks are 0 for $p = 0$ and about 0.03 for $p = 1$. When $p = 0$, the CTQW travels around the ring and interferes with itself. For the Kleinberg networks, we consider the clustering exponents $\alpha = 2$ [see Fig. 3(b)] and $\alpha = 3$ [see Fig. 3(c)] and we add q connections per node to the underlying ring. When we do not add any edges (i.e., $q = 0$), a Kleinberg network has a mean clustering coefficient of 0 and the evolution of the IPR resembles that in Fig. 3(a) for $p = 0$. For the Kleinberg networks with $\alpha = 2$ and $q = 1$, the IPR approaches values of about 0.05, hinting at localization. Visually inspecting the wave-function evolution confirms that the CTQW has a noticeably nonzero amplitude for only a few nodes in some of these networks. [See Fig. 5(a) in *Appendix B: Localization in Kleinberg and Holme–Kim networks*.] For the Kleinberg networks with $\alpha = 2$ and $q \geqslant 1$, the IPR approaches a smaller value as we increase q [see Fig. 3(b)]. For $\alpha = 2$, it is likely that the edge-addition process introduces some long-range edges, causing the CTQW to propagate through the whole network rather than being confined to a local region. (This is somewhat reminiscent of the appearance of new infection clusters via long-range edges in spreading processes on networks [59].) For $\alpha = 3$, the added edges are more likely to connect nearby nodes than to connect distant nodes. In this case, the IPR approaches values between 0.05 and 0.06 as we increase q [see Fig. 3(c)]. We believe that this is due to the existence of many local clusters in the networks. For both $\alpha = 2$ and $\alpha = 3$, the means of the mean clustering coefficients of the Kleinberg networks approach a value between 0.28 and 0.29 for $q = 4$. In the HK networks, for p' close to 1, we observe IPR values of up to 0.1 [see Fig. 3(d)]. This indicates that we observe localization, which is further evident in the evolution of individual wave functions. [See Fig. 5(b) in *Appendix B: Localization in Kleinberg and Holme–Kim networks*.] The means of the mean clustering coefficients of the HK networks are about 0.13 for $p' = 0$ and about 0.74 for $p' = 1$.

Conclusions and discussion. We examined how local clustering can induce localization of continuous-time quantum walks (CTQWs) on networks, and we thereby obtained insights into the influence of network structure on the long-time behavior of CTQWs. A key result is that local clustering can inhibit the propagation of CTQWs, which is relevant to consider when employing quantum walks in quantum communication channels [27]. We also illustrated that inverse participation ratio (IPR) is a useful indicator of localization of CTQWs on networks. However, identifying a universal IPR threshold that clearly distinguishes between localized and delocalized states is not straightforward, so it is also useful to visually inspect wave-function evolution.

Our findings motivate experimental studies of quantum-walk localization in clustered networks (e.g., using photonic implementations of quantum walks [60]). Such experiments can probe the role of local clustering in directing quantum-transport processes. In this context, it is worthwhile to study localization effects for potential applications of quantum walks in quantum memory, as localized quantum walks require less space than delocalized quantum walks to store and retrieve information [45].

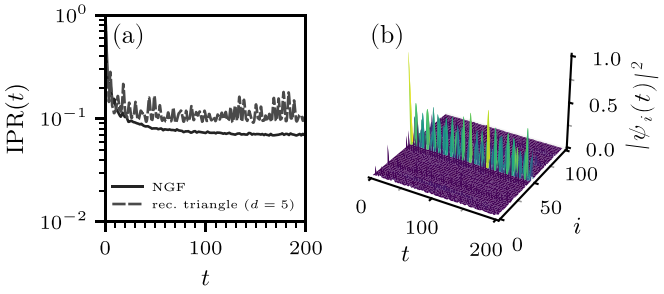

FIG. 4. Localization in networks that we construct using the network geometry with flavor (NGF) model. (a) Evolution of the IPR for both NGF networks (with $s = -1$) and a recursive triangle network with depth $d = 5$. For the NGF model, the curve is the mean of results for 1000 NGF networks, which each have 100 nodes. The CTQW starts at node 51 in the NGF networks. The recursive triangle network has 96 nodes; the CTQW starts at node 36, where localization is strongest. (b) Probability density $|\psi_i(t)|^2 = |\langle i|\psi(t)\rangle|^2$ as a function of the node i and time t for a CTQW that starts at node 51 in one 100-node NGF network (with $s = -1$).

Acknowledgment. L.B. acknowledges financial support from hessian.AI.

Data availability. Our code and simulation data are available at [61].

Appendix A: Localization in NGF networks. To examine the impact of randomness in network generation on recursive triangle networks, which are deterministic, we consider two-dimensional (2D) NGF networks with a flavor value of $s = -1$ [50,51,62]. In these NGF networks, a flavor value of $s = -1$ constrains each edge to be adjacent to at most two triangles. (NGF networks with other flavor values do not have this constraint.) Rather than attaching new triangles deterministically, the NGF model creates networks through a stochastic process. In our simulations, we set the model's inverse-temperature parameter to 0, which yields the Eden model [63] on a 2D simplicial complex [62].

In Fig. 4(a), we compare the evolution of the IPR for NGF networks with $s = -1$ and a recursive triangle network with depth $d = 5$. We average the IPR over 1000 NGF networks. In the NGF networks (which have 100 nodes), the CTQW starts at node 51. In the recursive triangle network (which has 96 nodes), the CTQW starts at node 36, where localization is strongest. The mean clustering coefficient of

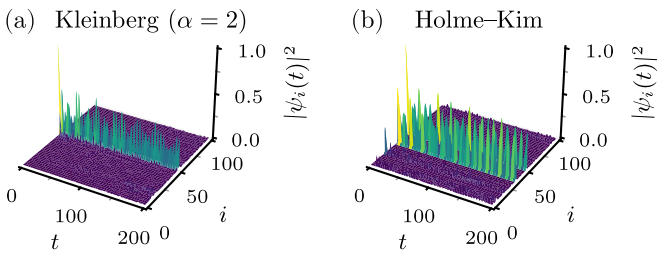

FIG. 5. Probability density $|\psi_i(t)|^2 = |\langle i|\psi(t)\rangle|^2$ as a function of the node i and time t for a CTQW that starts at node 51 in (a) a 100-node Kleinberg network with $\alpha = 2$ and $q = 1$ and (b) a 100-node Holme–Kim network with $p' = 1$.

these NGF networks is about 0.65, and it is about 0.69 for the recursive triangle network. The mean IPR for the NGF networks is similar in magnitude to the IPR for the recursive triangle network. To further illustrate localization dynamics, we plot the CTQW evolution on a single NGF network in Fig. 4(b). The randomness in the NGF generation process reduces the number of degenerate eigenvalues. (For example, the 100-node NGF network in Fig. 4(b) has one degenerate eigenvalue, whereas the 96-node recursive triangle network has 22 degenerate eigenvalues.) Consequently, the associated terms in Eq. (7) contribute less to the long-time mean IPR in NGF networks than in recursive triangle networks.

Appendix B: Localization in Kleinberg and Holme–Kim networks. To complement our findings on CTQW localization in Kleinberg navigable small-world networks and Holme–Kim networks, we plot (see Fig. 5) the probability density $|\psi_i(t)|^2$ as a function of the node i and time t for a CTQW that starts at node 51 in a 100-node Kleinberg network (with $\alpha = 2$ and $q = 1$) and a 100-node Holme–Kim network (with $p' = 1$).

[1] A. M. Childs and J. Goldstone, Spatial search by quantum walk, Phys. Rev. A **70**, 022314 (2004).

[2] F. Magniez, A. Nayak, J. Roland, and M. Santha, Search via quantum walk, SIAM J. Comput. **40**, 142 (2011).

[3] R. Portugal, *Quantum Walks and Search Algorithms* (Springer-Verlag, Heidelberg, Germany, 2013)

[4] H. Krovi, F. Magniez, M. Ozols, and J. Roland, Quantum walks can find a marked element on any graph, Algorithmica **74**, 851 (2016).

[5] A. Ambainis, Quantum walk algorithm for element distinctness, SIAM J. Comput. **37**, 210 (2007).

[6] E. Sánchez-Burillo, J. Duch, J. Gómez-Gardenes, and D. Zueco, Quantum navigation and ranking in complex networks, Sci. Rep. **2**, 605 (2012).

[7] L. Rossi, A. Torsello, and E. R. Hancock, Node centrality for continuous-time quantum walks, in *Proceedings of the Joint IAPR International Workshops on Statistical Techniques in Pattern Recognition (SPR) and Structural and Syntactic Pattern Recognition (SSPR)* (Springer-Verlag, Heidelberg, Germany, 2014), pp. 103–112.

[8] J. A. Izaac, X. Zhan, Z. Bian, K. Wang, J. Li, J. B. Wang, and P. Xue, Centrality measure based on continuous-time quantum walks and experimental realization, Phys. Rev. A **95**, 032318 (2017).

[9] S. Wald and L. Böttcher, From classical to quantum walks with stochastic resetting on networks, Phys. Rev. E **103**, 012122 (2021).

[10] L. Böttcher and M. A. Porter, Classical and quantum random-walk centrality measures in multilayer networks, SIAM J. Appl. Math. **81**, 2704 (2021).

[11] H. Tang, R. Shi, T.-S. He, Y.-Y. Zhu, T.-Y. Wang, M. Lee, and X.-M. Jin, TensorFlow solver for quantum PageRank in large-scale networks, Sci. Bull. **66**, 120 (2021).

[12] L. Böttcher and M. A. Porter, Complex networks with complex weights, Phys. Rev. E **109**, 024314 (2024).

[13] A. M. Childs, Universal computation by quantum walk, Phys. Rev. Lett. **102**, 180501 (2009).

[14] N. B. Lovett, S. Cooper, M. Everitt, M. Trevers, and V. Kendon, Universal quantum computation using the discrete-time quantum walk, Phys. Rev. A **81**, 042330 (2010).

[15] M. Mohseni, P. Rebentrost, S. Lloyd, and A. Aspuru-Guzik, Environment-assisted quantum walks in photosynthetic energy transfer, J. Chem. Phys. **129**, 174106 (2008).

[16] P. Rebentrost, M. Mohseni, I. Kassal, S. Lloyd, and A. Aspuru-Guzik, Environment-assisted quantum transport, New J. Phys. **11**, 033003 (2009).

[17] J. Nokkala, J. Piilo, and G. Bianconi, Complex quantum networks: A topical review, J. Phys. A: Math. Theor. **57**, 233001 (2024).

[18] J. Kempe, Quantum random walks: An introductory overview, Contemp. Phys. **44**, 307 (2003).

[19] S. Chakraborty, K. Luh, and J. Roland, How fast do quantum walks mix? Phys. Rev. Lett. **124**, 050501 (2020).

[20] V. Sood and P. Grassberger, Localization transition of biased random walks on random networks, Phys. Rev. Lett. **99**, 098701 (2007).

[21] Z. Burda, J. Duda, J.-M. Luck, and B. Waclaw, Localization of the maximal entropy random walk, Phys. Rev. Lett. **102**, 160602 (2009).

[22] A. V. Goltsev, S. N. Dorogovtsev, J. G. Oliveira, and J. F. F. Mendes, Localization and spreading of diseases in complex networks, Phys. Rev. Lett. **109**, 128702 (2012).

[23] P. Shukla and B. Bamieh, Localization phenomena in large-scale networked systems: Implications for fragility, IEEE Control Syst. Lett. **8**, 3087 (2024).

[24] P. Pradhan and A. Reza, Predicting steady-state behavior in complex networks with graph neural networks, Phys. Rev. E **112**, 054303 (2025).

[25] W. Chen, I. García-Mata, J. Martin, J. Gong, B. Georgeot, and G. Lemarié, Critical dynamics of the Anderson transition on small-world graphs, arXiv:2502.16884.

[26] O. Mülken, V. Pernice, and A. Blumen, Quantum transport on small-world networks: A continuous-time quantum walk approach, Phys. Rev. E **76**, 051125 (2007).

[27] J. P. Keating, N. Linden, J. C. F. Matthews, and A. Winter, Localization and its consequences for quantum walk algorithms and quantum communication, Phys. Rev. A **76**, 012315 (2007).

[28] S. R. Jackson, T. J. Khoo, and F. W. Strauch, Quantum walks on trees with disorder: Decay, diffusion, and localization, Phys. Rev. A **86**, 022335 (2012).

[29] R. Bueno and N. Hatano, Null-eigenvalue localization of quantum walks on complex networks, Phys. Rev. Res. **2**, 033185 (2020).

[30] A. Candeloro, L. Razzoli, S. Cavazzoni, P. Bordone, and M. G. A. Paris, Continuous-time quantum walks in the presence of a quadratic perturbation, Phys. Rev. A **102**, 042214 (2020).

[31] B. Tregenna, W. Flanagan, R. Maile, and V. Kendon, Controlling discrete quantum walks: Coins and initial states, New J. Phys. **5**, 83 (2003).

[32] N. Inui, Y. Konishi, and N. Konno, Localization of two-dimensional quantum walks, Phys. Rev. A **69**, 052323 (2004).

[33] N. Inui, N. Konno, and E. Segawa, One-dimensional three-state quantum walk, Phys. Rev. E **72**, 056112 (2005).
[34] K. Watabe, N. Kobayashi, M. Katori, and N. Konno, Limit distributions of two-dimensional quantum walks, Phys. Rev. A **77**, 062331 (2008).
[35] M. Štefaňák, I. Jex, and T. Kiss, Recurrence and Pólya number of quantum walks, Phys. Rev. Lett. **100**, 020501 (2008).
[36] A. Schreiber, K. N. Cassemiro, V. Potoček, A. Gábris, I. Jex, and C. Silberhorn, Decoherence and disorder in quantum walks: From ballistic spread to localization, Phys. Rev. Lett. **106**, 180403 (2011).
[37] A. H. Werner, Localization and recurrence in quantum walks, Ph.D. thesis, Gottfried Wilhelm Leibniz Universität Hannover, 2013, available at https://www.repo.uni-hannover.de/bitstream/123456789/8252/1/770599036.pdf.
[38] B. Kollár, T. Kiss, and I. Jex, Strongly trapped two-dimensional quantum walks, Phys. Rev. A **91**, 022308 (2015).
[39] C. Lyu, L. Yu, and S. Wu, Localization in quantum walks on a honeycomb network, Phys. Rev. A **92**, 052305 (2015).
[40] B. Danacı, İ. Yalçınkaya, B. Çakmak, G. Karpat, S. P. Kelly, and A. L. Subaşı, Disorder-free localization in quantum walks, Phys. Rev. A **103**, 022416 (2021).
[41] R. Sharma and S. Boettcher, Transport and localization in quantum walks on a random hierarchy of barriers, J. Phys. A: Math. Theor. **55**, 264001 (2022).
[42] R. Duda, M. N. Ivaki, I. Sahlberg, K. Pöyhönen, and T. Ojanen, Quantum walks on random lattices: Diffusion, localization, and the absence of parametric quantum speedup, Phys. Rev. Res. **5**, 023150 (2023).
[43] J. M. Kleinberg, The small-world phenomenon: An algorithmic perspective, in *Proceedings of the Thirty-Second Annual ACM Symposium on Theory of Computing, May 21–23, 2000, Portland, OR, USA*, edited by F. F. Yao and E. M. Luks (Association for Computing Machinery, New York City, NY, USA, 2000), pp. 163–170.
[44] P. Holme and B. J. Kim, Growing scale-free networks with tunable clustering, Phys. Rev. E **65**, 026107 (2002).
[45] C. M. Chandrashekar and T. Busch, Localized quantum walks as secured quantum memory, Europhys. Lett. **110**, 10005 (2015).
[46] M. Newman, *Networks*, 2nd ed. (Oxford University Press, Oxford, UK, 2018).
[47] M. Faccin, T. Johnson, J. Biamonte, S. Kais, and P. Migdał, Degree distribution in quantum walks on complex networks, Phys. Rev. X **3**, 041007 (2013).
[48] D. J. Thouless, Electrons in disordered systems and the theory of localization, Phys. Rep. **13**, 93 (1974).
[49] F. Wegner, Inverse participation ratio in $2+\varepsilon$ dimensions, Z. Phys. B **36**, 209 (1980).
[50] G. Bianconi and C. Rahmede, Network geometry with flavor: From complexity to quantum geometry, Phys. Rev. E **93**, 032315 (2016).
[51] G. Bianconi and C. Rahmede, Emergent hyperbolic network geometry, Sci. Rep. **7**, 41974 (2017).
[52] G. Bianconi and S. N. Dorogovtsev, The spectral dimension of simplicial complexes: A renormalization group theory, J. Stat. Mech. (2020) 014005.
[53] S. Dey, A. Chen, P. Basteiro, A. Fritzsche, M. Greiter, M. Kaminski, P. M. Lenggenhager, R. Meyer, R. Sorbello, A. Stegmaier, R. Thomale, J. Erdmenger, and I. Boettcher, Simulating holographic conformal field theories on hyperbolic lattices, Phys. Rev. Lett. **133**, 061603 (2024).
[54] A. Chen, J. Maciejko, and I. Boettcher, Anderson localization transition in disordered hyperbolic lattices, Phys. Rev. Lett. **133**, 066101 (2024).
[55] A. P. Millán, J. J. Torres, and G. Bianconi, Complex network geometry and frustrated synchronization, Sci. Rep. **8**, 9910 (2018).
[56] A. P. Millán, J. J. Torres, and G. Bianconi, Synchronization in network geometries with finite spectral dimension, Phys. Rev. E **99**, 022307 (2019).
[57] D. J. Watts and S. H. Strogatz, Collective dynamics of 'small-world' networks, Nature (London) **393**, 440 (1998).
[58] M. E. J. Newman and D. J. Watts, Renormalization group analysis of the small-world network model, Phys. Lett. A **263**, 341 (1999).
[59] D. Taylor, F. Klimm, H. A. Harrington, M. Kramár, K. Mischaikow, M. A. Porter, and P. J. Mucha, Topological data analysis of contagion maps for examining spreading processes on networks, Nat. Commun. **6**, 7723 (2015).
[60] H. Tang, X.-F. Lin, Z. Feng, J.-Y. Chen, J. Gao, K. Sun, C.-Y. Wang, P.-C. Lai, X.-Y. Xu, Y. Wang *et al.*, Experimental two-dimensional quantum walk on a photonic chip, Sci. Adv. **4**, eaat3174 (2018).
[61] L. Böttcher, Localization, GitLab repository, https://gitlab.com/ComputationalScience/localization.
[62] G. Bianconi and C. Rahmede, Complex quantum network manifolds in dimension $d > 2$ are scale-free, Sci. Rep. **5**, 13979 (2015).
[63] L. Böttcher and H. J. Herrmann, *Computational Statistical Physics* (Cambridge University Press, Cambridge, UK, 2021).